JOURNAL OF SOLID STATE CHEMISTRY 101, 331–339 (1992)

Structure Determination of $\alpha TiOSO_4$ from Powder X-ray Diffraction Data

IAN E. GREY*

CSIRO, Division of Mineral Products, P.O. Box 124, Port Melbourne, Victoria 3207, Australia

AND

ROBERT STRANGER

Department of Chemistry, University of Queensland, Queensland 4072, Australia

Received February 26, 1992; accepted May 19, 1992

$\alpha TiOSO_4$ forms as a leach-resistant phase during the digestion of altered ilmenite concentrates in concentrated sulphuric acid. It contains about 7 wt% Fe_2O_3 and its composition can be expressed as $Ti_{0.85}Fe_{0.15}O_{0.85}(OH)_{0.15}SO_4$. It has monoclinic symmetry, space group $C2/c$, and unit cell parameters $a = 5.1175(2)$, $b = 13.7675(6)$, $c = 9.5035(4)$ Å, $\beta = 91.097(3)°$. Its structure was determined using powder X-ray diffraction data and refined by the Rietveld method to $R_{wp} = 0.059$, $R_B = 0.022$, goodness of fit = 1.56 for 706 reflections to $2\theta = 140°$, Cu$K\alpha$ radiation. The structure comprises a 3-D framework of corner-linked $Ti1O_6$ and $Ti2O_6$ octahedra and SO_4 tetrahedra, with six-sided channels running parallel to both [100] and [001]. Alternating corner-shared octahedra and tetrahedra form four-member rings which link together into ribbons via the constituent octahedra. Ribbons containing $Ti1O_6$ and $Ti2O_6$ octahedra lie along [001] and [100], respectively, and differ in the relative positions of the pairs of vertices forming the four-member rings. Structural relationships between $\alpha TiOSO_4$ and other phases containing corner-linked octahedra and tetrahedra are described.

Introduction

In the depressed world commodities market of the 1990s, titania pigment production capacity continues to expand and is currently in excess of 3 million tpa, with applications mainly in paints, paper, and plastics. The strong demand for titania pigments relates to their properties of high refractive index (high opacity, whiteness, and brightness factors), chemical inertness, and resistance to photochemical degradation. About 50% of titania pigments are produced by the sulfate process. This involves digestion of titanium-bearing minerals in concentrated sulphuric acid to form a solid oxysulphate cake, followed by leaching of the cake in dilute acid and hydrolysis to precipitate titania (*1*). Traditionally ilmenite, $FeTiO_3$, has been the sulfate process feedstock but problems associated with the disposal of iron sulfates has led to the increased use of high-titania feedstocks such as titania slag and to an interest in the development of ilmenite

* To whom correspondence should be addressed.

0022-4596/92 $5.00

upgrading processes to produce an acid-soluble high-titania product (*2*).

As part of a project to produce acid-soluble titania from ilmenite, we constructed a laboratory-scale digestion apparatus to measure the potential plant solubility of various ilmenite concentrates and their upgraded products. For certain samples it was found that digestion temperatures above ~180°C led to the formation of a white, leach-resistant product and resulted in incomplete titanium extraction. The powder X-ray diffraction pattern for the insoluble phase closely matched published (unindexed) patterns for synthetic mixed sulphates of Ti^{4+} with trivalent cations Fe^{3+}, Al^{3+}, and Cr^{3+} (*3*, *4*). The composition of these phases was presented in the form $TiO_2 \cdot (0.08–0.1)M_2O_3 \cdot (1.3–1.4)SO_3$ (*4*). More recently, Samoilova *et al.* have shown that a phase with the same XRD pattern as that for the mixed sulfates could be prepared as a metastable phase in the TiO_2–SO_3–H_2O system (*5*). It was formed within the stability field for $TiOSO_4$ and was designated as $\alpha TiOSO_4$.

We report here the ab initio structure determination of the leach-resistant phase from powder diffraction data, the refinement of the structure by the Rietveld method, and the structural relationships to other phases.

Experimental

A commercial ilmenite concentrate from Western Australia was ground (100% −45 μm) and mixed with 98% H_2SO_4 at an acid : ore w/w ratio of 1.6. The mixture was contained in a glass reaction vessel immersed in an oil bath and stirred with a stainless steel impeller. The temperature was raised to 80°C, and 10% H_2SO_4 was added to lower the acid strength to 92% and to set off the exothermic sulfation reactions. The temperature rose to a maximum value of 190°C. The slurry progressively thickened and formed a solid cake which was baked at 195°C for 4 hr. It was then chipped out of the reactor, crushed to −2 mm, and leached with stirring in 10% H_2SO_4 for 6 hr at 60°C. The insoluble grey-white residue remaining was filtered, washed with 20% H_2SO_4 and then de-ionized water, and dried at 105°C. Chemical analyses of the residue gave 41.0 wt% TiO_2, 7.4 wt% Fe_2O_3, 43.5 wt% SO_3, 0.1 wt% Al_2O_3, 0.03 wt% Cr_2O_3, and 1.96 wt% SiO_2.

X-ray powder diffraction patterns were recorded using a Philips PW1050 goniometer-/PW1710 controller operated with Cu $K\alpha$ radiation at 40 kV and 40 mA and fitted with 1° divergence, receiving, and scatter slits. The samples were side-loaded to minimize preferred orientation effects. Intensity measurements were made at intervals of 0.025° 2θ. One data collection was made from 10° to 90°, using a fixed step-counting time of 5 sec, to provide data for the unit cell and structure determinations. A second data set was collected from 15° to 140° using a variable step-counting time strategy (*6*) with counting times ranging from 0.9 to 10.9 sec. This procedure was used to compensate for intensity falloff with angle and thus to improve the relative counting statistics of high-angle reflections for refinements using the Rietveld (*7*) method.

The pattern deconvolution program PROFIT (H. Scott, private communication) was used to obtain individual integrated intensities from the powder pattern. The program UNITCELL, employing the Visser method (*8*), was used to determine the unit cell. The SHELX76 package (*9*) was used for obtaining Patterson and Fourier maps and for preliminary refinements. Profile refinements were made using the Rietveld analysis program RIET-7, a modified version of the codes of Hill and Howard (*10*) and Wiles and Young (*11*). The background was defined by a four-parameter polynomial in $2\theta^n$, where $n = 0–3$. A 2θ-variable pseudo-Voigt peak shape function (*10*) was

used. The peak full-width at half-maximum (FWHM) function was of the form $FWHM^2 = U \tan^2\theta + V \tan\theta + W$ (12) and was calculated for 5.0 half-widths on either side of the peak maximum. Neutral atom scattering factors, including anomalous dispersion corrections, were taken from Ref. (*13*).

Electron diffraction patterns were obtained using Philips 400X and JEOL 4000 FX transmission electron microscopes. For these studies the powdered sample was dispersed in acetone and collected on holey carbon copper grids.

Structure Determination and Refinement

Application of the automatic indexing program, UNITCELL, to 30 reflections with $2\theta < 50°$ yielded a C-centred monoclinic cell with $a = 5.11, b = 13.75, c = 9.50$ Å, $\beta = 91.1°$. The unit cell was subsequently confirmed from electron diffraction patterns, which also showed extinctions due to a *c*-glide, consistent with space groups $C2/c$ and Cc. Using indexing based on this unit cell the reflection list was progressively expanded to 56 reflections. The unit cell parameters were refined and input to the pattern deconvolution program PROFIT, together with the fixed-step counting-time diffraction profile. The profile deconvolution was initially limited to $2\theta < 60°$ because of quite severe peak overlap at higher angles. The resulting 89 integrated intensities from PROFIT were corrected for multiplicity and Lorentz polarization and were reduced to structure factors, which were then used to calculate a Patterson map.

After some unsuccessful attempts to establish a model in $C2/c$, a change was made to the noncentrosymmetric space group Cc. The coordinates of four Ti, S atoms were established from the Patterson map, and the positions of five oxygen atoms were subsequently located in Fourier maps. This provided enough information to build a partial structure, to distinguish the titanium and sulphur atoms, and to estimate the positions of the remaining five oxygens needed to complete the SO_4 and TiO_6 polyhedra. Location of the remaining oxygen atoms in difference Fourier maps was only possible when the 2θ range used for the reflections was expanded beyond 60°, i.e., to $d < 1.54$ Å. This can be explained by the fact that phase information from the individual atoms of the SO_4 tetrahedra is lost when the data set is terminated at *d* values greater than the S–O distances (S–O < 1.5 Å). As discussed by Oppenheim (14), the Fourier synthesis of a structure from the diffraction data is very sensitive to the phases but is insensitive to the magnitudes of the diffracted intensities. In terms of structure determination using powder data this means that more structural information can be obtained if high-angle data from the pattern deconvolution are included, despite the loss of accuracy concerning the intensities because of increasing overlap problems (in PROFIT, groups of peaks that cannot be resolved are given equal intensities).

The model obtained was refined using the fixed-time Rietveld data set, $2\theta = 10°–90°$. An inspection of the refined atom coordinates showed that the atoms were close to a centrosymmetric distribution. An appropriate origin shift was introduced and the atom coordinates of pairs of atoms were averaged to give a starting model in space group $C2/c$.

The centrosymmetric model was then refined using the variable-time Rietveld data set, $2\theta = 15°–140°$. The refinement converged smoothly. The final refinement involved 19 atom coordinates, 4 isotropic temperature factors (a common B value was refined for the oxygen atoms), 1 scale factor, 1 zero point parameter, 4 cell parameters, 3 half-width parameters, 1 asymmetry parameter, 4 background parameters, and 3 pseudo-Voigt shape-angular-variation parameters. The agreement indices were $R_{wp} = 0.059$, $R_B = 0.022$, and goodness of fit =

TABLE I

RIETVELD REFINEMENT RESULTS FOR $\alpha TiOSO_4$

Unit Cell Parameters

$a = 5.1175(2)$, $b = 13.7675(6)$, $c = 9.5035(4)$ Å, $\beta = 91.097(3)°$

Atomic coordinates and B (Å^2) values

Atom	x	y	z	B (Å^2)
Ti 1	$\frac{1}{2}$	0.0810(3)	$\frac{1}{4}$	1.5(1)
Ti 2	$\frac{3}{4}$	$\frac{1}{4}$	0	1.7(1)
S	0.2588(8)	0.3904(3)	0.0677(4)	0.37(7)
O 1	0.484(2)	0.3506(7)	0.4156(9)	0.46(9)
O 2	0.271(2)	0.0666(6)	0.0765(9)	0.46
O 3	0.222(2)	0.4669(7)	0.1725(9)	0.46
O 4	0.284(2)	0.1678(7)	0.3384(9)	0.46
O 5	0.055(2)	0.3192(6)	0.0931(8)	0.46

Agreement indices

$R_p = 0.059$, $R_{wp} = 0.059$, $R_B = 0.022$, goodness of fit = 1.56

1.56 for 706 reflections. The refined unit cell parameters, atomic coordinates, and isotropic thermal parameters are given in Table I. The observed, calculated, and difference profiles are shown in Fig. 1.

From the structure refinement the numbers of atoms found in the unit cell were 8 M (Ti + Fe), 8 S, and 40 O, consistent with a formula $MOSO_4$, $Z = 8$. The Ti and Fe atoms could not be distinguished in the refinement. The substitution of Fe^{3+} for Ti^4 in the above formula gives a charge imbalance. Charge balance is most likely achieved by substitution of OH^- for O^{2-}, giving a solid solution of the type $(TiOSO_4)_x(FeOHSO_4)_{1-x}$, $x \sim 0.85$. Alternative means of charge balance, such as anion vacancies or metal interstitials, were not identified in the structure analysis. For consistency with previous work (*5*), the new phase will be referred to as $\alpha TiOSO_4$.

Structure Description and Relationship to Other Structures

Projections of the structure along [100] and [001] are given in Figs. 2 and 3, respectively. They show that the structure consists of a three-dimensional framework of corner-shared TiO_6 octahedra and SO_4 tetrahedra. There are two independent metal atoms at sites of point symmetry 2 (Ti1) and $\bar{1}$ (Ti2). The $Ti1O_6$ octahedra share *trans* vertices with $Ti2O_6$, while the $Ti2O_6$ octahedra share *cis* vertices with $Ti1O_6$, resulting in zig-zag chains of corner-shared octahedra approximately along [201] and [20$\bar{1}$]. The remaining four vertices of both octahedra are shared with SO_4 tetrahedra.

Bond lengths and angles for the polyhedra are given in Table II. The sulfate tetrahedron is regular and has a mean bond length of 1.46 Å compared with 1.47 Å for the sum of the ionic radii (*15*). The O4 oxygen involved in corner sharing between octahedra is undersaturated and the Ti-O4 bonds are considerably shortened. However there is no tendency toward formation of a titanyl ion as occurs for vanadium in similar compounds, e.g., $\beta VOPO_4$, V–O = 1.57 Å (*16*). The mean Ti–O bond length for both octahedra, 1.98 Å, is consistent with that expected for Ti^{4+} with some substitution by Fe^{3+} (*17*).

A striking feature of the structure is the presence of six-sided channels running parallel to both the a and c axes. Both channels are bounded by four octahedral edges and two tetrahedral edges but the sequence of edges is different, being o,t,o,o,o,t for the [100] channels and o,o,t,o,o,t for the [001] channels. Despite the appearance of openness conveyed by the channels, the structure is in fact densely packed, as indicated by the anion packing index of 16.73 Å^3/O^{2-}. This compares with a value of 16.4 Å^3/O^{2-} for $MoOPO_4$ which has cations of similar size to those in $\alpha TiOSO_4$ and has the oxygen atoms in a slightly distorted cubic close-packed arrangement (*18*).

Figure 2 reveals a close relationship of the polyhedral topology in $\alpha TiOSO_4$ to that in the "pinwheel" structures, as exemplified by merwinite, $Ca_3Mg[SiO_4]_2$ (*19*). Figure 4 shows the pseudohexagonal (100) layer of

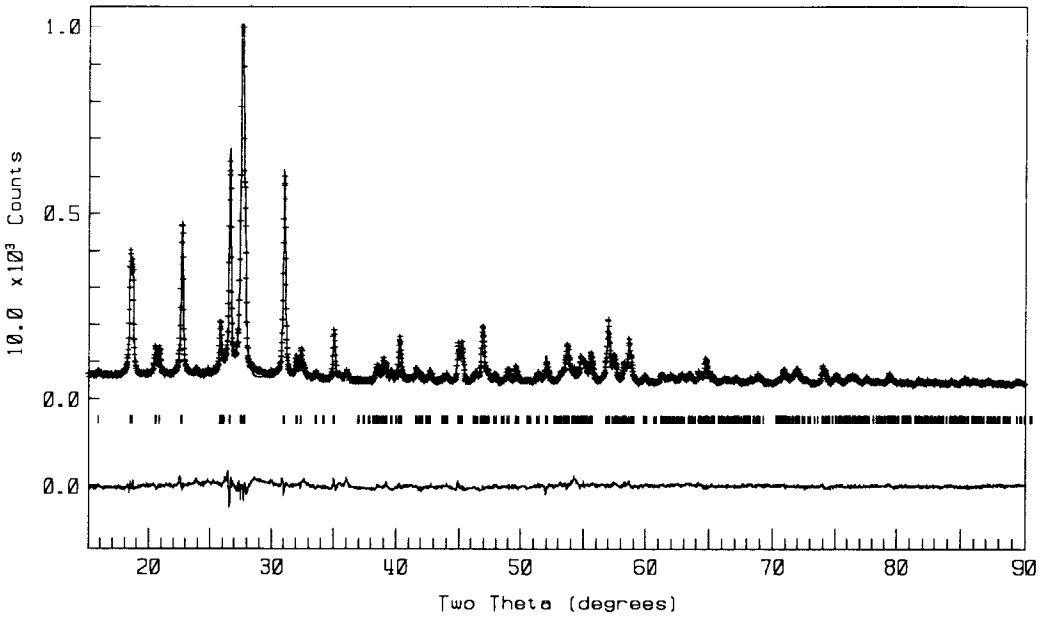

FIG. 1. Observed, calculated, and difference X-ray powder diffraction profile for $\alpha TiOSO_4$, truncated at $2\theta = 90°$ to show the high-intensity data more clearly. The observed data are indicated by points and the calculated profile by the continuous line. Positions of Bragg reflections are shown by tick marks.

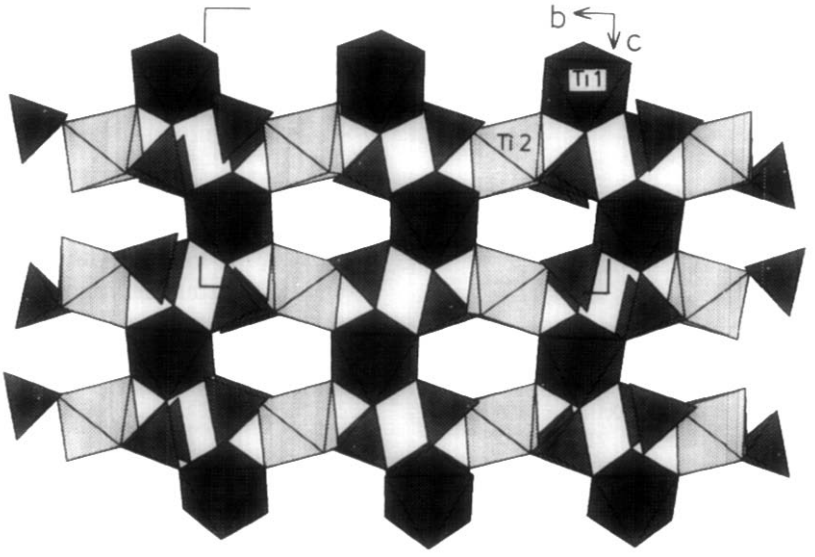

FIG. 2. Polyhedral representation of the structure of $\alpha TiOSO_4$ viewed along [100]. The TiO_6 and SO_4 polyhedra are heavily shaded to emphasise the [001] ribbons of alternating octahedra and four-member rings.

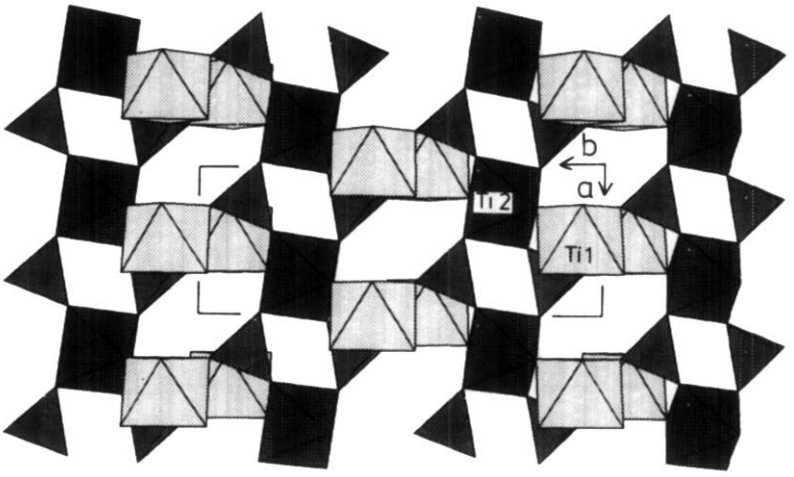

FIG. 3. Polyhedral representation of the structure of $\alpha TiOSO_4$ viewed along [001]. The $Ti2O_6$ and SO_4 polyhedra are heavily shaded to emphasise the [100] 5-Å ribbons of alternating octahedra and four-member rings.

octahedra and tetrahedra in merwinite, with composition $Mg[SiO_4]_2$. The [001] ribbons of octahedra connected by pairs of corner-linked tetrahedra in merwinite have a direct counterpart in $\alpha TiOSO_4$, shown by the heavily shaded polyhedral ribbons along [001] in Fig. 2. The corner linking of the octahedra and tetrahedra in the ribbons gives four-member rings separated by the constituent octahedra. In merwinite the [001] ribbons constitute the structural repeat unit in the (100) planes and connect to one another along [010] via corner sharing between octahedra and tetrahedra. In $\alpha TiOSO_4$ the ribbons are separated by individual $Ti2O_6$ octahedra which corner link to both the $Ti1O_6$ and SO_4 in the [001] ribbons. The (100) layer composition in $\alpha TiOSO_4$ is then $2 \cdot Ti1O_{2/2}[S_2O_6O_{2/2}] + 2 \cdot Ti2O_{4/2} = 4 \cdot TiOSO_4$.

TABLE II

BOND LENGTHS (Å) AND ANGLES (°) IN $ATiOSO_4$

	M–O (Å)	Range of O–O (Å)	Range of O–*M*–O (°)
Ti1–O4 (×2)	1.84(1)	2.73(2)–2.85(1)	87.1(4)–99.1(7)
Ti1–O2 (×2)	2.014(9)		168.7(6)–171.0(4)
Ti1–O3 (×2)	2.08(1)		
Ti2–O4 (×2)	1.918(9)	2.74(1)–2.90(1)	87.8(4)–92.2(4)
Ti2–O1 (×2)	2.01(1)		180.0
Ti2–O5 (×2)	2.018(9)		
S–O1	1.43(1)	2.32(1)–2.43(1)	105.6(6)–112.6(6)
S–O5	1.45(1)		
S–O3	1.464(9)		
S–O2	1.50(1)		

M–*M* distances (Å) less than 4 Å

Ti1–S 3.297(4), 3.425(6) Ti2–S 3.245(4), 3.296(4)
Ti1–Ti2 3.579(4)

The $Ti2O_6$ octahedra also form ribbons by corner linking to pairs of tetrahedra as illustrated in Fig. 3. The ribbons lie along [100] and are thus orthogonal to those involving the $Ti1O_6$ octahedra. In contrast to the undulating chains of octahedra and four-member rings in the ribbons involving $Ti1O_6$, those involving $Ti2O_6$ comprise linear chains, with a 5-Å repeat along [100]. The linear 5-Å ribbons of composition $MO_{2/2}[X_2O_6O_{2/2}]$ are a common structural component of $MOXO_4$ structures and many other mixed octahedral–tetrahedral structures. In merwinite-type structures, for example, these ribbons lie along [010] (and

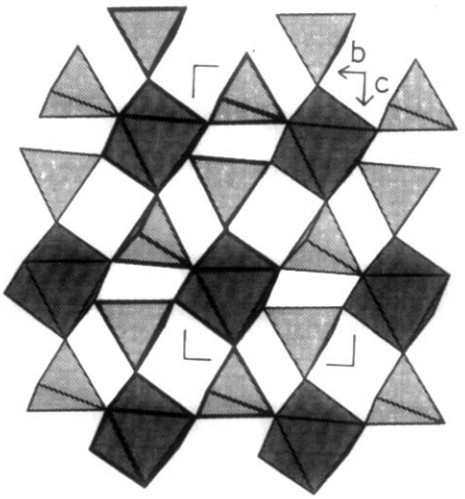

FIG. 4. Polyhedral representation of a (100) layer of octahedra and tetrahedra in merwinite, $Ca_3Mg[SiO_4]_2$ (*19*). A [001] ribbon of alternating octahedra and four-member rings is heavily outlined for ease of comparison with the ribbons in Fig. 1.

equivalent pseudohexagonal directions) as shown in Fig. 4. In $BaTi_2(P_2O_7)_2$ the linking of such ribbons into a 3-D framework involves corner sharing of PO_4 tetrahedra in adjacent ribbons (*20*). The composition of the ribbons is thus $MO_{2/2}[X_2O_4O_{4/2}]$ in this compound.

In $\alpha TiOSO_4$ the *trans* vertices of $Ti2O_6$ normal to the 5-Å ribbons are corner-linked to $Ti1O_6$ octahedra. There is thus a topological relationship of the 5-Å ribbons to the ReO_3 structure. This is illustrated in Figs. 5a and 5b. As in ReO_3-related structures such as the perovskites, the corner-linked ribbons of octahedra and tetrahedra have great structural flexibility, through tilting and rotation, to accommodate compositional variations. For example, the $GeOHPO_4$ structure comprises 5-Å ribbons directed along [110] and [1$\bar{1}$0] in successive (001) planes, and rotation of the polyhedra in these ribbons about [001] allows this structure type to adapt to a wide range of relative sizes of octahedra and tetrahedra and to accept extra cations in "stuffed derivatives" such as titanite, $Ca[TiOSiO_4]$, and lazulite, $Mg[AlOHPO_4]_2$ (*21*). In $MoOPO_4$ and related structures, intersecting [11$\bar{0}$] and [1$\bar{1}$0] ribbons form undulating (001) planes that link together by octahedral corner sharing along [001] (*18*). In these and other $M(O,OH)XO_4$ structures the structural description usually focuses on the chains of corner-linked octahedra, rather than on the 5-Å ribbons of alternating four-member rings and octahedra. However, the octahedral chains do not always maintain their integrity, due either to large displacements of the cations toward one of the corner-shared vertices to form square pyramidal coordination as in $\beta VOPO_4$ (*16*) or to complete separation of the corner-linked octahedra as in natisite, $Na_2[TiOSiO_4]$ (*22*). Natisite has a structure related to that of $MoOPO_4$, in which the (001) planes containing the ⟨110⟩ ribbons (in this case composed of SiO_4 tetrahedra and TiO_5 square pyramids) alternate with the planes of sodium atoms.

It is of interest to compare the structure of $\alpha TiOSO_4$ to that of the other known $TiOSO_4$ polymorph, which has orthorhombic symmetry with cell parameters $a = 6.340$, $b = 10.936$, $c = 5.150$ Å (*23*). Although the

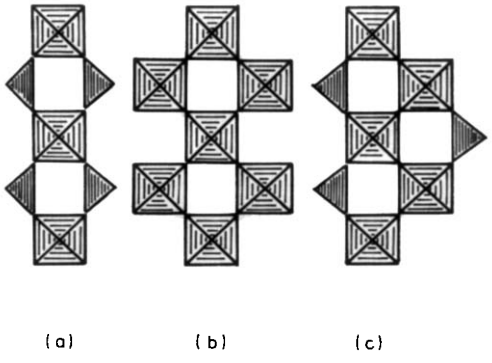

FIG. 5. (a) 5-Å ribbon of octahedra and tetrahedra as in $\alpha TiOSO_4$. (b) Equivalent topology of corner-shared octahedra as in ReO_3. (c) Composite 5-Å ribbon in $\beta NbOPO_4$ (*25*) and $TiOSO_4 \cdot H_2O$ (*27*).

structure of $TiOSO_4$ has not been reported, it has a powder pattern and unit cell dimensions similar to those reported by Levin and Roth for $\beta NbOPO_4$ (*24*). The structure of this phase has recently been determined by Raveau and colleagues (*25*). They showed that $\beta NbOPO_4$ was the $m = 2$ member of a homologous series $(PO_2)_4(MO_3)_{2m}$ (M = W, Nb) for which the structures are composed of ReO_3 slabs separated by layers containing PO_4 tetrahedra. The basic structure repeating unit in $\beta NbOPO_4$ is a ribbon of corner-shared octahedra and tetrahedra with a 5-Å repeat along [010]. This is illustrated in Fig. 5c, where it is seen to be a composite of the 5-Å ribbon in $\alpha TiOSO_4$ and the ReO_3 structure, having a two-octahedra-wide strip of corner-shared octahedra. In $\beta NbOPO_4$ the ReO_3 segments do not extend out of the 5-Å ribbons, whereas in higher m homologues further octahedral corner-sharing to octahedra above and below the plane occurs (*26*). The structure of $TiOSO_4 \cdot H_2O$ also contains 5-Å ribbons of the type shown in Fig. 5c (*27*).

A puzzling feature of $\alpha TiOSO_4$ is that the iron content appears to be relatively constant, both in our preparations using a variety of natural ilmenite-starting products and in those of the Russian workers using synthetic mixtures of hydrated titanium oxide and ferric oxide (*3*), yet the [Fe]/[Ti] atomic ratio of 0.15 to 0.20 has no obvious origin in the cation ordering in the structure. Other trivalent cations such as Cr^{3+} and Al^{3+} substitute in $\alpha TiOSO_4$ at the same atomic ratio as for Fe^{3+} (*4*). Although the preparation of $\alpha TiOSO_4$ has been reported without trivalent cations, it is metastable and readily transforms to other phases (*5*). A possible explanation is related to the fact that in the pure titanium compound, quite severe local charge imbalances occur at the different anion sites. The anion O4 is shared between two TiO_6 octahedra and has a Pauling valence sum of 1.33, while O1–O3 and O5, shared between TiO_6 and SO_4, have valence sums of 2.17. Charge balanced substitutions of the type $M^{3+} + OH \leftrightarrow Ti^{4+} + O^{2-}$ provide local electroneutrality when the OH substitutes for O4. The observed M^{3+}/Ti^{4+} ratio perhaps represents a type of threshold for 3-D continuity between the $M(OH)SO_4$ regions of local electroneutrality which relieve the strain associated with the $TiOSO_4$ regions.

In ongoing studies of H_2SO_4 digestion of titaniferous minerals we have observed that digestion of altered ilmenites gives another oxysulfate with composition $Ti_xFe_{1-x}O_x(OH)_{1-x}SO_4$ having higher values of x than in $\alpha TiOSO_4$. Preliminary XRD and electron diffraction studies show that this phase has a structure related to that of $Ge(OH)PO_4$ (*21*).

Acknowledgments

We thank M. Perroux, CNRS laboratoire de Cristallographie, Grenoble, and T. White, University of Queensland, for obtaining electron diffraction patterns, and I. Madsen and N. Scarlett for help with the data collections. Our thanks also to M. Lanyon for carrying out the H_2SO_4 digestion tests.

References

1. J. Barksdale, "Titanium. Its Occurrence, Chemistry, and Technology." 2nd ed., Ronald Press, New York (1966).
2. I. D. Martin and H. W. Hockin, "Production of Anosovite from Titaniferous Materials," U.S. Patent No. 3,502,460 (March 1970).
3. L. I. Bekkerman, I. N. Zabrodin, and A. I. Sheinkman, *Russ. J. Appl. Chem.* **46,** 1421 (1973).
4. L. I. Bekkerman and I. N. Zabrodin, *Russ. J. Inorg. Chem.* **17,** 1245 (1972).
5. G. G. Samoilova, I. I. Kalinichenko, and R. M. Sadykov, *Russ. J. Inorg. Chem.* **31,** 801 (1986).
6. I. C. Madsen and R. J. Hill, *Adv. X-Ray Anal.*, in press (1992).
7. H. M. Rietveld, *J. Appl. Crystallogr.*, **2,** 65 (1969).
8. R. Garvey, "UNITCELL. A Personal Computer Program for Finding Lattice Parameters from Powder Data," North Dakota State University.
9. G. M. Sheldrick, "SHELX-76, Program for

Crystal Structure Determination," University of Cambridge, U.K. (1976).
10. R. J. HILL AND C. J. HOWARD, "Australian Atomic Energy Commission Report No. M112," AAEC (now ANSTO), Lucas Heights, New South Wales, Australia (1986).
11. D. B. WILES AND R. A. YOUNG, *J. Appl. Crystallogr.* **14,** 149 (1981).
12. G. CAGLIOTTI, A. PAOLETTI, AND F. P. RICCI, *Nucl. Instrum.* **3,** 223 (1958).
13. "International Tables for X-ray Crystallography," Vol. IV, Kynoch Press, Birmingham, U.K. (1974).
14. A. V. OPPENHEIM, *Proc. Inst. Electr. Electron. Eng.* **69,** 529 (1981).
15. R. D. SHANNON AND C. T. PREWITT, *Acta Crystallogr.* **B25,** 925 (1969).
16. R. GOPAL AND C. CALVO, *J. Solid State Chem.* **5,** 432 (1972).
17. I. E. GREY, A. COLLOMB, AND X. OBRADORS, *J. Solid State Chem.* **91,** 131 (1991).
18. P. KIERKEGAARD AND M. WESTERLUND, *Acta Chem. Scand.* **18,** 2217 (1964).
19. P. B. MOORE AND T. ARAKI, *Am. Mineral.* **57,** 1355 (1972).
20. S. WANG AND S. J. HWU, *J. Solid State Chem.* **90,** 31 (1991).
21. H. MAYER AND H. VOLLENKLE, *Z. Kristallogr.* **136,** 387 (1972).
22. H. NYMAN, M. O'KEEFE, AND J. O. BOVIN, *Acta Crystallogr.* **B34,** 905 (1978).
23. S. NAKA, K. TANAKA, Y. SUWA, AND Y. TAKEDA, *J. Inorg. Nucl. Chem.* **39,** 1239 (1977).
24. E. M. LEVIN AND R. S. ROTH, *J. Solid State Chem.* **2,** 250 (1970).
25. A. LECLAIRE, H. CHAHBOUN, D. GROULT, AND B. RAVEAU, *Z. Kristallogr.* **177,** 277 (1986).
26. B. DOMENGES, F. STUDER, AND B. RAVEAU, *Mat. Res. Bull.* **18,** 669 (1983).
27. G. LUNDGREN, *Ark. Kemi* **10,** 397 (1956).